

Electrically Conductive Coordination Polymer for Highly Selective Chemiresistive Sensing of Volatile Amines

Siping Wang,^{†,§} Jie Liu,^{‡,§} Hongmei Zhao,[†] Zhifen Guo,[†] Hongzhu Xing,^{*,†,§} and Yuan Gao^{*,‡}[†]Provincial Key Laboratory of Advanced Energy Materials, College of Chemistry, Northeast Normal University, Renmin Street 5268, Changchun 130024, China[‡]State Key Laboratory on Integrated Optoelectronics, College of Electronic Science and Engineering, Jilin University, Qianjin Street 2699, Changchun 130012, China

Supporting Information

ABSTRACT: A new electrically conductive coordination polymer is synthesized using anthracene-incorporated organic ligand. The compound exhibits a band-like structure and long-range π - π stacking of ligand. Interestingly, the fabricated chemiresistor using this coordination polymer shows selective sensing behavior for volatile amine detection with characteristics of quick response, good reproducibility, and room-temperature operation. This study not only presents a rare example of electrically conductive coordination polymer but also illustrates the useful application of coordination polymer for chemiresistor.

The prospective use of coordination polymers (CPs), also known as metal–organic frameworks (MOFs),^{1–3} in a number of desirable technologies, such as fuel cells,⁴ supercapacitors,⁵ electroluminescence,⁶ thermoelectrics,⁷ and resistive sensing,^{8,9} greatly prompts research on conductive CPs.^{10,11} However, CPs are typically poor electrical conductors due to the poor orbital overlap between metal ions and organic ligands; hence, a vast majority of CPs do not provide a long-range charge transport pathway and behave as electrical insulators.^{10,12} One possible approach for electrically conductive CPs is long-range charge transport through inorganic chain units which can be considered as reduced counterparts of semiconductive metal oxides and metal chalcogenides, etc.¹³ Alternatively, long-range charge transport between electroactive organic ligand through a noncovalent interaction, such as π - π stacking, is another feasible strategy to realize electrical conductivity of CPs.^{14,15} It is exciting that tens of electrically conductive CPs have been synthesized on the basis of these approaches.¹⁰ Also, some of the conducting CPs display the potential application of gas sensing which is very important considering individual health, homeland security, and environmental concerns.^{16,17} However, CP-based chemiresistor is still scarcely reported to date owing to the aforementioned poor electrical conductivity as shown by CPs.^{8–10}

In this work, a new 1D electrically conductive CP **1** is rationally synthesized using electroactive anthracene-based ligand. The compound features a unique band-like structure and shows abundant uncoordinated carboxyl groups in the framework. Interestingly, **1** is demonstrated to be a useful

chemiresistive sensing material for the detection of volatile amines.

The anthracene-incorporated organic ligand of 5,5'-(anthracene-9,10-diylbis(ethyne-2,1-diyl))diisophthalic acid (**L**) was synthesized via Sonogashira coupling reaction according to a reported procedure (Supporting Information).¹⁸ Needle-like crystals of **1** were synthesized by reaction of $\text{Cd}(\text{NO}_3)_2 \cdot 4\text{H}_2\text{O}$ and ligand in DMF at 100 °C. Single-crystal X-ray diffraction reveals that **1** crystallizes in triclinic space group $P\bar{1}$ with a formula of $[\text{Cd}(\text{H}_2\text{L})_2] \cdot 3\text{H}_2\text{O} \cdot 2\text{DMF}$. The asymmetric unit contains two Cd ions, two ligands, two DMF molecules, and three water molecules (Figure S1 in the Supporting Information). The two crystallographically unique Cd ions, Cd(1) and Cd(2), in the structure are both heptacoordinated by oxygen atoms. The Cd–O bond lengths range from 2.227(2) to 2.501(3) Å. As shown in Figure 1a, the Cd(1) ion locates on the edge of the band-like framework, while the Cd(2) ion locates in the middle of the band-like framework. Two adjacent Cd(2) ions are further connected by

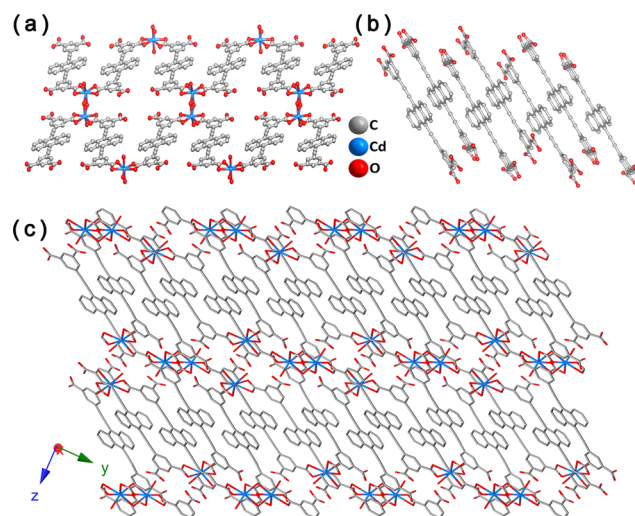


Figure 1. Crystal structure of **1**. (a) A perspective view shows double-band framework. (b) The long-range π - π stacking of ligands in the structure. (c) An overview of the structure. Hydrogen atoms and DMF molecules are omitted for clarity.

Received: September 25, 2017

a Cd–O–Cd bond to form a dimer unit. As shown in Figure 1c, these band-like chains are further self-assembled through π – π interaction between ligands (Figure 1b) to construct a three-dimensional supramolecular structure of **1**. The face-to-face distances between ligands are 3.653 and 3.902 Å, respectively.

The bulk sample of **1** was first characterized by powder X-ray diffraction (PXRD), where the experimental pattern matches well with the simulated one, indicating good purity of the synthesized material (Figure S2). Thermogravimetric (TG) analysis under air atmosphere displays a two-step weight loss where the coordinated DMF and water molecules (expt 13.1 wt %; calcd 13.0 wt %) are removed before 240 °C, followed by organic ligand decomposition (expt 68.1 wt %; calcd 69.7 wt %) at ca. 370–530 °C (Figure S3). PXRD study suggests the residual is CdO after complete removal of organic ligand at 550 °C (Figure S4). Fourier transform infrared (FTIR) spectroscopy (Figure S5) exhibits a characteristic peak from the alkynyl group in the ligand at 2200 cm^{-1} . The strong peaks at ca. 1545 and 1436 cm^{-1} are due to vibrations of the carboxylate groups in the ligand, and the peak at ca. 759 cm^{-1} can be ascribed to the out-of-plane bending vibration of the C–H bond in benzene groups of the ligand. The vibration of a coordinated H_2O molecule is observed at ca. 3375 cm^{-1} . The intense peak for carbonyl stretching at ca. 1650 cm^{-1} ($\nu_{\text{C=O}}$) suggests the presence of a DMF molecule. In addition, weak peaks around 3000 cm^{-1} would associate with the vibrations of C–H bonds in DMF molecule.^{19,20}

It is intriguing that long-range π – π stacking of anthracene-based ligands is observed in **1**, which provides a potential charge transport pathway in the structure. The crystal indexing experiment suggests that the stacking of ligand in the structure is parallel to the long axis of the crystal (Figure S6). As shown in Figure 2, the electrical conductivity of solvated **1** was measured by two-probe method using single-crystal sample where it was immobilized between two blocks of conducting silver resin to support Ohmic contact. The electrical conductive performances of different crystals were measured by sweeping voltage under ambient conditions (Supporting Information). To compare the electrical conductivity in various crystals, I – V curves are transformed into J – E curves, i.e., current density (J) versus electric field strength (E), by considering the length and the cross-sectional area of the conduction channel for each sample. As shown in Figure 2c, the tested crystals exhibit very similar conductive behavior. The obtained average electrical conductivity of **1** is about $1.27 \times 10^{-6} \text{ S cm}^{-1}$. This value is very close to that shown by other electrically conductive coordination polymers, including $[\text{Ni}(\text{6-MP})_2 \cdot 2\text{H}_2\text{O}]_n$,²¹ $[\text{Cu}_2\text{Br}(\text{IN})_2]_n$,²² $\{\text{Cu}(\text{TANC})\} \cdot \text{F}_{0.5}\}_n$,²³ $[\{\text{Rh}_2(\text{acam})_4\}_2\text{I}]_n \cdot 6n\text{H}_2\text{O}$,²⁴ and $[\text{Ni}(\text{6-ThioG})_2 \cdot 2\text{H}_2\text{O}]_n$.²¹

Structural analysis suggests that half of the carboxyl (C(=O)OH) groups in **1** are uncoordinated; hence, they might serve as antenna to interact with guest molecules leading to desirable sensing applications. With **1** showing high electrical conductivity, the use of **1** for chemiresistive sensing is preferred. The chemiresistor was then fabricated by coating a finely ground sample on an alumina tube (Supporting Information). A static system was applied to investigate the gas sensing behavior of the fabricated sensor under air atmosphere (30% RH) at room temperature (Figure S7).²⁵ The sensing performance is evaluated on the basis of response values calculated from variation of its resistance.

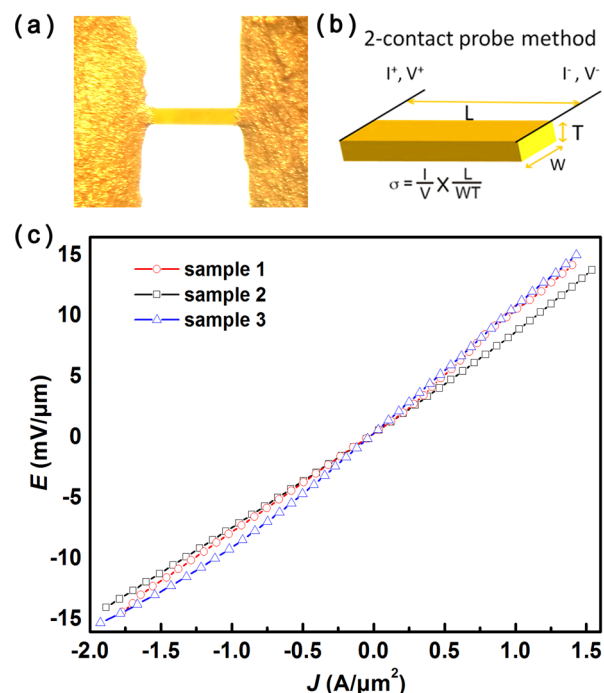


Figure 2. (a) The optical image of **1** (the contacts are made by silver resins, and the length between contacts is ca. 360 μm). (b) Two-probe method for conductivity measurement where I , V , L , W , and T represent working current and voltage, and length, width, and thickness of sample, respectively. (c) J – E curves of **1** measured from different crystal samples.

Organic amines were first chosen for the sensing of volatile organic compounds (VOCs), owing to their high risk for human health, universal usage in production and experiment, as well as high volatility. As shown in Figure 3a, the sensor is capable of ethylenediamine (EDA) detection where the resistance of the sensor significantly decreases in the presence of EDA vapor. The response value becomes larger as the gas concentration increases and reaches saturation at high EDA

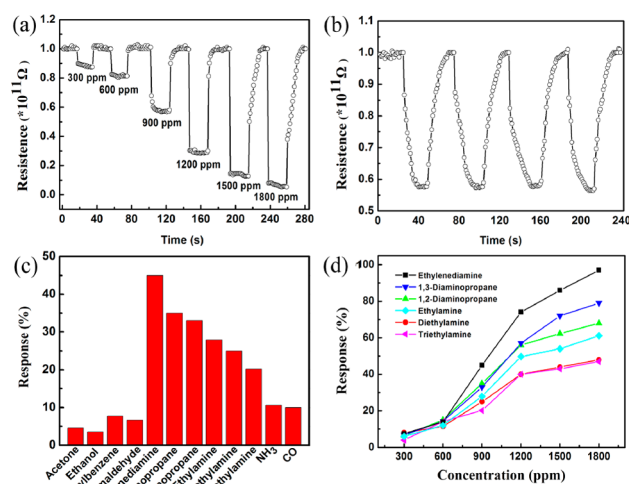


Figure 3. Gas sensing performance of the MOF sensor. (a) Dynamic resistance variation at different EDA concentrations. (b) Reproducibility curve for EDA (900 ppm) sensing. (c) Responses for different VOCs at 900 ppm. (d) Relationship between response and gas concentration for volatile amines.

concentrations. Such behavior is similar to that shown by chemiresistors fabricated from metal oxides. It is believed that more amine molecules are in contact with the sensor under higher gas concentration, resulting in an increase of response, whereas after a dynamic equilibrium between gas and sensor is achieved, the sensor comes into a saturation state.²⁶

The response time at moderate EDA concentration is less than 3 s, and the corresponding recovery time is less than 10 s, where the response time and the recovery time are defined as time required decreasing the saturated resistance to its 10% and time required increasing the resistance to 90% saturation value, respectively.^{27,28} These response times are comparable and even shorter than that needed by commercialized chemiresistors of metal oxides.²⁹ Figure 3b shows the performance of the sensor based on instantaneous supply and cut of EDA, where the sensor shows good response repeatability. PXRD and SEM study suggests that amine treatment does not change the structure and the morphology of **1** (Figures S2 and S8). Besides, the sensor is stable enough to survive for two months under ambient conditions (Figure S9).

Beyond EDA, the chemiresistive sensing for other VOCs with different functional groups and polarities was further studied under air atmosphere. As shown in Figure 3c, the sensor is highly selective for volatile amine detection, showing a more significant response than for other VOCs. It is believed that a strong hydrogen bonding interaction between the carboxyl group and amine plays a crucial role for the selectivity. The hydrogen bond is universal in various chemical and biological systems,^{30–33} where polar groups, such as $-\text{NH}_2$ and $-\text{OH}$ groups,^{34,35} can get very close to each other and experience an unusually strong electrostatic interaction. Actually, the utilization of a hydrogen bonding interaction to achieve chemical selectivity has widely been reported in fields of molecular recognition and sensing.^{36,37} As compared with VOCs including formaldehyde, acetone, and methanol, etc., organic amine shows larger polarity due to the more electronegative amino group. Hence it might interact with a carboxyl group in a relatively strong hydrogen bond.

The sensing performances of different volatile amines are displayed in Figure 3d. The efficiencies for chosen amines are in the trend $\text{EDA} > 1,3\text{-diaminopropane} \geq 1,2\text{-propanediamine} > \text{ethylamine} > \text{diethylamine} \geq \text{triethylamine}$. This can be understood according to the characteristic of the hydrogen bond; i.e., the strength of the hydrogen bond is directionally affected. The primary amine possesses a polar amino group on the side of the molecule, which makes it easier to spatially interact with carboxylate groups through the hydrogen bond. In contrast, secondary and tertiary amines, such as diethylamine and triethylamine, with an amino group in the middle of the molecule, would interact with the MOF structure in weaker hydrogen bonding. By the same argument, it is rational that a linear EDA molecule exhibits a higher sensing response than bending 1,2-diaminopropane and 1,3-propanediamine molecules. Beyond the hydrogen bonding interaction, the proton from the neutral carboxyl group may transmit to amine to form an ionic species. This might contribute the high response for amine sensing through an electrostatic force, and the ionic species may affect the electrical conductivity in the MOF compound. In contrast, VOCs such as acetone, CO, and ethanol, etc., cannot provide this possibility.

In summary, a novel conductive CP is synthesized using an electroactive anthracene-based organic ligand. The com-

pound features a band-like framework and long-range $\pi-\pi$ stacking of ligand in the structure. The CP is then investigated for sensing VOCs, making use of the uncoordinated carboxyl groups in the structure as an antenna. The fabricated chemiresistor shows selective sensing behavior for amine detection with the characteristics of a rapid response, good reproducibility, and room-temperature operation. This work demonstrates that conductive CPs are promising materials for gas sensing applications, and we are hopeful that more and more conductive MOFs could be synthesized and applied for useful electrical applications.

■ ASSOCIATED CONTENT

📄 Supporting Information

The Supporting Information is available free of charge on the ACS Publications website at DOI: 10.1021/acs.inorgchem.7b02464.

Detailed experimental procedures, analytical data, SEM images, PXRD patterns, UV-vis spectra, IR spectra, scheme of sensing, and X-ray crystallographic data (PDF)

Accession Codes

CCDC 1517717 contains the supplementary crystallographic data for this paper. These data can be obtained free of charge via www.ccdc.cam.ac.uk/data_request/cif, or by emailing data_request@ccdc.cam.ac.uk, or by contacting The Cambridge Crystallographic Data Centre, 12 Union Road, Cambridge CB2 1EZ, UK; fax: +44 1223 336033.

■ AUTHOR INFORMATION

Corresponding Authors

*E-mail: xinghz223@nenu.edu.cn

*E-mail: gaoyuan@jlu.edu.cn

ORCID

Hongzhu Xing: 0000-0001-7179-0394

Author Contributions

[§]S.W. and J.L. contributed equally.

Notes

The authors declare no competing financial interest.

■ ACKNOWLEDGMENTS

This work is supported by the National Natural Science Foundation of China (21473024 and 61520106003) and Science and Technology Research Project of Jilin Province (JJKH20170906KJ).

■ REFERENCES

- (1) Kitagawa, S.; Kitaura, R.; Noro, S. I. Functional Porous Coordination Polymers. *Angew. Chem., Int. Ed.* **2004**, *43*, 2334–2375.
- (2) Yaghi, O. M.; Li, G.; Li, H. Selective Binding and Removal of Guests in A Microporous Metal–Organic Framework. *Nature* **1995**, *378*, 703–7206.
- (3) Rieth, A. J.; Tulchinsky, Y.; Dincă, M. High and Reversible Ammonia Uptake in Mesoporous Azolate Metal–Organic Frameworks with Open Mn, Co, and Ni Sites. *J. Am. Chem. Soc.* **2016**, *138*, 9401–9404.
- (4) Tan, A. D.; Wang, Y. F.; Fu, Z. Y.; Tsiakaras, P.; Liang, Z. X. Highly effective oxygen reduction reaction electrocatalysis: Nitrogen-doped hierarchically mesoporous carbon derived from interpenetrated nonporous metal-organic frameworks. *Applied Catalysis B. Appl. Catal., B* **2017**, *218*, 260–266.

- (5) Lee, S. H.; Choi, S. Bimetallic zeolitic imidazolate frameworks for symmetric electrical double-layer supercapacitors with aqueous electrolytes. *Mater. Lett.* **2017**, *207*, 129–132.
- (6) Huang, H.; Beuchel, M.; Park, Y.; Baesjou, P. J.; Meskers, S. C. J.; de Leeuw, D. M.; Asadi, K. Solvent-Induced Galvanoluminescence of Metal–Organic Framework Electroluminescent Diodes. *J. Phys. Chem. C* **2016**, *120*, 11045–11048.
- (7) Dolgoplova, E. A.; Brandt, A. J.; Ejegbavwo, O. A.; Duke, A. S.; Maddumapatabandi, T. D.; Galhenage, R. P.; Larson, B. W.; Reid, O. G.; Ammal, S. C.; Heyden, A.; Chandrashekhar, M.; Stavila, V.; Chen, D. A.; Shustova, N. B. Electronic Properties of Bimetallic Metal–Organic Frameworks (MOFs): Tailoring the Density of Electronic States through MOF Modularity. *J. Am. Chem. Soc.* **2017**, *139*, 5201–5209.
- (8) Campbell, M. G.; Sheberla, D.; Liu, S. F.; Swager, T. M.; Dincă, M. $\text{Cu}_3(\text{hexaiminotriphenylene})_2$: An Electrically Conductive 2D Metal–Organic Framework for Chemiresistive Sensing. *Angew. Chem., Int. Ed.* **2015**, *54*, 4349–4352.
- (9) Campbell, M. G.; Liu, S. F.; Swager, T. M.; Dincă, M. Chemiresistive Sensor Arrays from Conductive 2D Metal–Organic Frameworks. *J. Am. Chem. Soc.* **2015**, *137*, 13780–13783.
- (10) Sun, L.; Campbell, M. G.; Dincă, M. Electrically Conductive Porous Metal–Organic Frameworks. *Angew. Chem., Int. Ed.* **2016**, *55*, 3566–3579.
- (11) Rubio-Martínez, M.; Puigmartí-Luis, J.; Imaz, I.; Dittrich, P.; Maspocho, D. Dual-Template[™] Synthesis of One-Dimensional Conductive Nanoparticle Superstructures from Coordination Metal–Peptide Polymer Crystals. *Small* **2013**, *9*, 4160–4167.
- (12) Givaja, G.; Amo-Ochoa, P.; Gómez-García, C.; Zamora, F. Coordination polymers with nucleobases: Electrical conductive coordination polymers. *Chem. Soc. Rev.* **2012**, *41*, 115–147.
- (13) Sun, L.; Hendon, C. H.; Minier, M. A.; Walsh, A.; Dincă, M. Million-Fold Electrical Conductivity Enhancement in $\text{Fe}_2(\text{DEBDC})$ versus $\text{Mn}_2(\text{DEBDC})$ ($E = \text{S}, \text{O}$). *J. Am. Chem. Soc.* **2015**, *137*, 6164–6167.
- (14) Musumeci, C.; Osella, S.; Ferlauto, L.; Niedzialek, D.; Grisanti, L.; Bonacchi, S.; Jouaiti, A.; Milita, S.; Ciesielski, A.; Beljonne, D.; Hosseini, M. W.; Samori, P. Influence of the supramolecular order on the electrical properties of 1D coordination polymers based materials. *Nanoscale* **2016**, *8*, 2386–2394.
- (15) Chen, D.; Xing, H.; Su, Z.; Wang, C. Electrical conductivity and electroluminescence of a new anthracene-based metal–organic framework with p-conjugated zigzag chains. *Chem. Commun.* **2016**, *52*, 2019–2022.
- (16) Gómez-Herrero, J.; Zamora, F. Coordination Polymers for Nanoelectronics. *Adv. Mater.* **2011**, *23*, 5311–5317.
- (17) Gentili, D.; Givaja, G.; Mas-Balleste, R.; Azani, M.; Shehu, A.; Leonardi, F.; Mateo-Martí, E.; Greco, P.; Zamora, F.; Cavallini, M. Patterned conductive nanostructures from reversible self-assembly of 1D coordination polymer. *Chem. Sci.* **2012**, *3*, 2047–2051.
- (18) Li, X.; Chen, D.; Liu, Y.; Yu, Z.; Xia, Q.; Xing, H.; Sun, W. Anthracene-based indium metal–organic framework as a promising photosensitizer for visible-light-induced atom transfer radical polymerization. *CrystEngComm* **2016**, *18*, 3696–3702.
- (19) Falaise, C.; Volkringer, C.; Loiseau, T. Mixed Formate-Dicarboxylate Coordination Polymers with Tetravalent Uranium: Occurrence of Tetranuclear $\{\text{U}_4\text{O}_4\}$ and Hexanuclear $\{\text{U}_6\text{O}_4(\text{OH})_4\}$ Motifs. *Cryst. Growth Des.* **2013**, *13*, 3225–3231.
- (20) Pretsch, E.; Bühlmann, P.; Badertscher, M. *Introduction to Structure Determination of Organic Compounds*, 4th revised and enlarged ed; Springer-Verlag: Berlin, 2009; pp 49–70.
- (21) Amo-Ochoa, P.; Castillo, O.; Alexandre, S.; Welte, L.; de Pablo, P.; Rodríguez-Tapiador, M.; Gómez-Herrero, J.; Zamora, F. Synthesis of Designed Conductive One-Dimensional Coordination Polymers of Ni(II) with 6-Mercaptopurine and 6-Thioguanine. *Inorg. Chem.* **2009**, *48*, 7931–7936.
- (22) Amo-Ochoa, P.; Welte, L.; González-Prieto, R.; Sanz Miguel, P. J.; Gómez-García, C. J.; Mateo-Martí, E.; Delgado, S.; Gómez-Herrero, J.; Zamora, F. Single layers of a multifunctional laminar Cu(I,II) coordination polymer. *Chem. Commun.* **2010**, *46*, 3262–3264.
- (23) Tadokoro, M.; Yasuzuka, S.; Nakamura, M.; Shinoda, T.; Tatenuma, T.; Mitsumi, M.; Ozawa, Y.; Toriumi, K.; Yoshino, H.; Shiomu, D.; Sato, K.; Takui, T.; Mori, T.; Murata, K. A High-Conductivity Crystal Containing a Copper(I) Coordination Polymer Bridged by the Organic Acceptor TANC. *Angew. Chem., Int. Ed.* **2006**, *45*, 5144–5147.
- (24) Fuma, Y.; Ebihara, M.; Kutsumizu, S.; Kawamura, T. A Diamondoid Network of Tetrakis(acetamidato)dirhodium in Mixed Oxidation States Linked by μ_4 -Iodide Having a 10^5 Enhancement of Its Electrical Conductivity by Water Molecules of Hydration. *J. Am. Chem. Soc.* **2004**, *126*, 12238–12239.
- (25) Xiao, Y.; Yang, Q.; Wang, Z.; Zhang, R.; Gao, Y.; Sun, P.; Sun, Y.; Lu, G. Improvement of NO_2 gas sensing performance based on discoid tin oxide modified by reduced graphene oxide. *Sens. Actuators, B* **2016**, *227*, 419–426.
- (26) Qu, F.; Jiang, H.; Yang, M. Designed formation through a metal organic framework route of $\text{ZnO}/\text{ZnCo}_2\text{O}_4$ hollow core–shell nanocages with enhanced gas sensing properties. *Nanoscale* **2016**, *8*, 16349–16356.
- (27) Yao, M. S.; Tang, W. X.; Wang, G. E.; Nath, B.; Xu, G. MOF Thin Film-Coated Metal Oxide Nanowire Array: Significantly Improved Chemiresistor Sensor Performance. *Adv. Mater.* **2016**, *28*, 5229–5234.
- (28) Drobek, M.; Kim, J. H.; Bechelany, M.; Vallicari, C.; Julbe, A.; Kim, S. S. MOF-Based Membrane Encapsulated ZnO Nanowires for Enhanced Gas Sensor Selectivity. *ACS Appl. Mater. Interfaces* **2016**, *8*, 8323–8328.
- (29) Qu, F.; Yuan, Y.; Guarecuco, R.; Yang, M. Low Working-Temperature Acetone Vapor Sensor Based on Zinc Nitride and Oxide Hybrid Composites. *Small* **2016**, *12*, 3128–3133.
- (30) Cannizzaro, C. E.; Houk, K. N. Magnitudes and Chemical Consequences of $\text{R}_3\text{N}^+-\text{C}-\text{H}\cdots\text{O}=\text{C}$ Hydrogen Bonding. *J. Am. Chem. Soc.* **2002**, *124*, 7163–7169.
- (31) Wu, G.; Yamada, K.; Dong, S.; Grondy, H. Intermolecular Hydrogen-Bonding Effects on the Amide Oxygen Electric-Field-Gradient and Chemical Shielding Tensors of Benzamide. *J. Am. Chem. Soc.* **2000**, *122*, 4215–4216.
- (32) Matsumoto, K.; Ozawa, T.; Jitsukawa, K.; Masuda, H. Synthesis, Solution Behavior, Thermal Stability, and Biological Activity of an Fe(III) Complex of an Artificial Siderophore with Intramolecular Hydrogen Bonding Networks. *Inorg. Chem.* **2004**, *43*, 8538–8546.
- (33) Manna, U.; Patil, S. Self-Assembly of Biopolymers on Colloidal Particles via Hydrogen Bonding. *J. Phys. Chem. Lett.* **2010**, *1*, 907–911.
- (34) Kollman, P. A.; Allen, L. C. The Theory of The Hydrogen Bond. *Chem. Rev.* **1972**, *72*, 283–303.
- (35) Grabowski, S. J. Hydrogen bonding strength—measures based on geometric and topological parameters. *J. Phys. Org. Chem.* **2004**, *17*, 18–31.
- (36) Grate, J. W. Hydrogen-Bond Acidic Polymers for Chemical Vapor Sensing. *Chem. Rev.* **2008**, *108*, 726–745.
- (37) Ahmed, I.; Jung, S. H. Applications of metal-organic frameworks in adsorption/separation processes via hydrogen bonding interactions. *Chem. Eng. J.* **2017**, *310*, 197–215.